

Production of Ultracold, Polar RbCs* Molecules via Photoassociation

Andrew J. Kerman,¹ Jeremy M. Sage,¹ Sunil Sainis,¹ Thomas Bergeman,² and David DeMille¹

¹*Department of Physics, Yale University, New Haven, CT 06520, USA*

²*Department of Physics and Astronomy, SUNY, Stony Brook, NY 11794-3800, USA*

(Dated: November 11, 2018)

We have produced ultracold, polar RbCs* molecules via photoassociation in a laser-cooled mixture of Rb and Cs atoms. Using a model of the RbCs* molecular interaction which reproduces the observed rovibrational structure, we infer decay rates in our experiments into deeply bound $X^1\Sigma^+$ ground state RbCs vibrational levels as high as $5 \times 10^5 \text{ s}^{-1}$ per level. Population in such deeply bound levels could be efficiently transferred to the vibrational ground state using a single stimulated Raman transition, opening the possibility to create large samples of stable, ultracold polar molecules.

PACS numbers: 32.80.Pj, 33.20.-t, 33.80.Ps, 34.20.-b, 34.50.Gb, 34.50.Rk

Ultracold polar molecules, due to their strong, long-range, anisotropic dipole-dipole interactions, may provide access to qualitatively new regimes previously inaccessible to ultracold atomic and molecular systems. For example, they might be used as the qubits of a scalable quantum computer [1]. New types of highly-correlated many-body quantum states could become accessible such as BCS-like superfluids [2], supersolid and checkerboard states [3], or “electronic” liquid crystal phases [4]. Ultracold chemical reactions between polar molecules have been discussed [5], and might be controlled using electric fields [6]. Finally, the sensitivity of current molecule-based searches for violations of fundamental symmetries [7] might be increased to unprecedented levels.

Cold, trapped polar molecules have so far only been produced using either buffer-gas cooling [8] or Stark-slowing [9], at temperatures of ~ 10 - 100 mK [8, 9]. This is much higher than the ~ 1 - 100 μK accessible with atoms, and attempts to bridge this gap with evaporative cooling may run afoul of predicted molecular Feshbach resonances [10] or inelastic losses [11].

Another approach is to extend well-known techniques for producing ultracold (non-polar) homonuclear diatomic molecules in binary collisions of ultracold atoms, either through photoassociation [12, 13, 14, 15, 16], or Feshbach resonance [17, 18]. In these methods, the translational and rotational temperatures of the molecules are limited only by the initial atomic sample, possibly providing access all the way to the quantum-degenerate regime [15, 18]. An important limitation, however, is that the molecules are typically formed in weakly bound vibrational levels near dissociation, which may have vanishing electric dipole moments [19], and are unstable with respect to inelastic collisions [10, 11, 15]; therefore, a method for transferring them to the vibrational ground state is desirable [14].

Several authors have discussed the extension of these methods to the formation of (heteronuclear) polar molecules in collisions between different atomic species [20, 21, 22, 23]. In recent experiments NaCs⁺ and RbCs⁺ ions formed in the presence of near-resonant light have in-

deed been observed in small numbers [21]; however, these observations did not permit an analysis of their formation mechanism, nor demonstrate a method for producing neutral, ultracold polar molecules.

In this Letter, we describe the production of electronically excited, polar RbCs* molecules via photoassociation in an ultracold ($T \sim 100 \mu\text{K}$) mixture of ⁸⁵Rb and ¹³³Cs atoms. We have observed their electronic, vibrational, rotational, and hyperfine structure, as well as the large DC Stark effect characteristic of a polar molecule. Analysis of our data allows us to infer spontaneous decay rates to deeply bound vibrational levels of the RbCs $X^1\Sigma^+$ electronic ground state of up to $\sim 5 \times 10^5 \text{ s}^{-1}$ per level. Our calculations show that molecules in such levels could be transferred to the vibrational ground state of RbCs with a single, stimulated Raman transition.

Photoassociation (PA), illustrated in Fig. 1, occurs when two colliding ground state atoms absorb a photon and are promoted to a weakly bound, electronically excited molecular level [24, 25]. As indicated in Fig. 1(b), the levels accessed in heteronuclear PA are of much shorter range than their homonuclear counterparts; this arises from the fact that at long range, in their first excited state, two identical atoms interact via the resonant-dipole interaction (with potential $V(R) \propto R^{-3}$), whereas two atoms of different species interact only via much shorter-ranged van der Waals forces ($V(R) \propto R^{-6}$) [20, 26]. In the latter case, for a given excited-state binding energy, the Franck-Condon factor (FCF) characterizing the overlap between the initial free-atom ground state and the excited molecular bound state is significantly smaller, requiring a higher PA intensity. However, the FCF for decay to deeply bound vibrational levels of the ground $X^1\Sigma^+$ state is also larger, as we discuss below.

Our observations are made in a dual-species magneto-optical trap (MOT) [27]. We excite colliding atoms into RbCs* rovibrational levels at a variable detuning Δ below the lowest lying excited asymptote, correlating to Rb $5S_{1/2} + \text{Cs } 6P_{1/2}$ (this is the most favorable choice for our purposes since these levels do not predissociate [28]). Af-

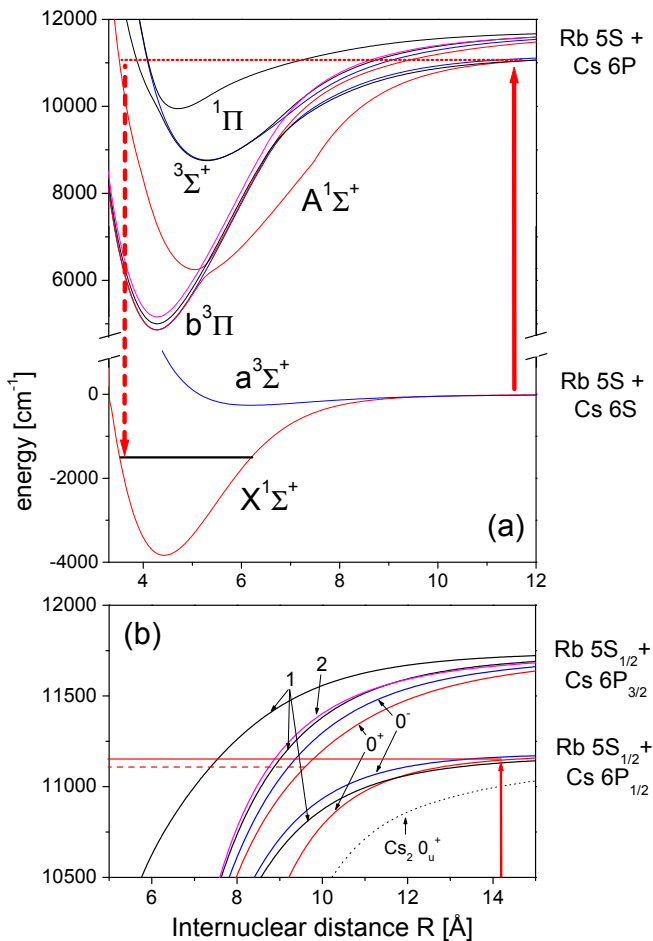


FIG. 1: (Color online) Schematic of the photoassociation process. (a) $^{85}\text{Rb} + ^{133}\text{Cs}$ atom pairs are excited during a collision (upward arrow) to molecular levels (horizontal line) below the Rb $5S_{1/2} + \text{Cs } 6P_{1/2}$ atomic asymptote. They can then decay (dashed, downward-pointing arrow) to ground state molecular levels. (b) Detailed view of the potentials, labelled by their Hund's case (c) quantum number $\Omega = 0^+, 0^-, 1, 2$. The horizontal lines indicate vibrational levels accessed in this work. The dotted curve shows the potential for the 0_u^+ state of Cs_2 , to illustrate its longer range character for weakly bound levels.

ter a pair is excited, it decays either to a ground-state RbCs molecule, or back to energetic free Rb and Cs atoms which typically escape from the two traps. The signature of RbCs* formation is then a resonant steady-state depletion of both the Rb and Cs traps induced by the PA laser. For optimal sensitivity, we maximize the PA-induced loss rate (proportional to the product of the Rb and Cs densities integrated over the PA beam profile) while minimizing other intrinsic losses that compete with it to determine the steady-state trap populations. For this purpose, we use forced dark-spot MOTs [29, 30] to increase the Rb and Cs densities by factors of 9 and 4 (relative to “bright” MOTs), respectively, while reducing their intrinsic losses due to light-assisted inelastic collisions [30]. These losses are further reduced in the Rb trap

by significantly decreasing the trapping laser intensity.

The peak density n , atom number N , and spatial overlap of the two atomic clouds were optimized using two-color absorptive imaging from two orthogonal directions. Typical values were: $N_{\text{Rb}} = 4 \times 10^8$, $n_{\text{Rb}} = 7 \times 10^{11} \text{ cm}^{-3}$, and $N_{\text{Cs}} = 3 \times 10^8$, $n_{\text{Cs}} = 3 \times 10^{11} \text{ cm}^{-3}$. Independent measurements of $N_{\text{Rb,Cs}}$ using resonance fluorescence confirmed these values to within $\sim 30\%$. Temperatures of $T_{\text{Rb}} = 55 \mu\text{K}$ and $T_{\text{Cs}} = 140 \mu\text{K}$ were measured using time-of-flight absorption imaging [35].

The Ti:sapphire PA laser produced 600 mW of power around 895 nm; its frequency was monitored using both a wavemeter and an optical spectrum analyzer, providing absolute (relative) accuracy of 150 MHz (5 MHz). To increase the PA intensity, the laser light was modematched into a build-up cavity (finesse ~ 60) placed around the vacuum chamber; its e^{-2} mode radius at the atom traps of $380 \mu\text{m}$ (the typical size of the MOT clouds was $750 \mu\text{m}$) resulted in PA intensities up to $4 \times 10^7 \text{ W/m}^2$ [27].

In order to detect PA-induced loss, the fluorescence rate of each MOT was monitored with a photodiode, as the frequency of the PA laser was scanned. An example of the observed signals is shown in Fig. 2, where the features common to both Rb and Cs traces can be identified as RbCs* states. From the depletion of the Rb trap (up to 70%) we estimate resonant heteronuclear PA rates as large as $\sim 1.5 \times 10^8 \text{ s}^{-1}$, close to the expected maximum rate for our parameters determined by probability conservation in a binary scattering process (the so-called “unitarity limit”) [25, 27]. The loss rates are indeed observed to saturate as a function of intensity, at values typically $> 10^6 \text{ W/m}^2$, significantly higher than in homonuclear experiments [22, 24]. These values are also consistent with our estimates based on a WKB approximation for the ground-state wavefunction at short range [20, 25, 27].

We have observed RbCs* levels over the range $\Delta \sim 10 \rightarrow 100 \text{ cm}^{-1}$ [27], and we find vibrational progressions corresponding to the expected $\Omega = 0^+, 0^-, 1$, and 2 potentials dissociating to both the $6P_{1/2}$ and $6P_{3/2}$ limits, as shown in Fig 1(b). The $\Omega = 0^\pm$ levels have no hyperfine splitting in leading order, and are thus identified by their clean rotational structure [Fig 2(a)]. The $\Omega = 1, 2$ features display a complex hyperfine-rotational structure, [Fig. 2(b)], the analysis of which is in progress.

We have also demonstrated the polar nature of the observed RbCs* states by applying electric fields [Fig 3]. The observed Stark effect agrees in form with that expected for a polar, diatomic rigid rotor, as illustrated by the fit in Fig 3. From this fit we extract an electric dipole moment for this level of $\mu_e = 1.3 \pm 0.1$ Debye.

We have analyzed our observations of the $\Omega = 0^\pm$ levels by fitting them to a model of the RbCs* potentials, based on *ab initio* calculations [31] and previous spectroscopic data [27, 32]. A thorough discussion of this analysis will be presented elsewhere. Fig. 4 shows a

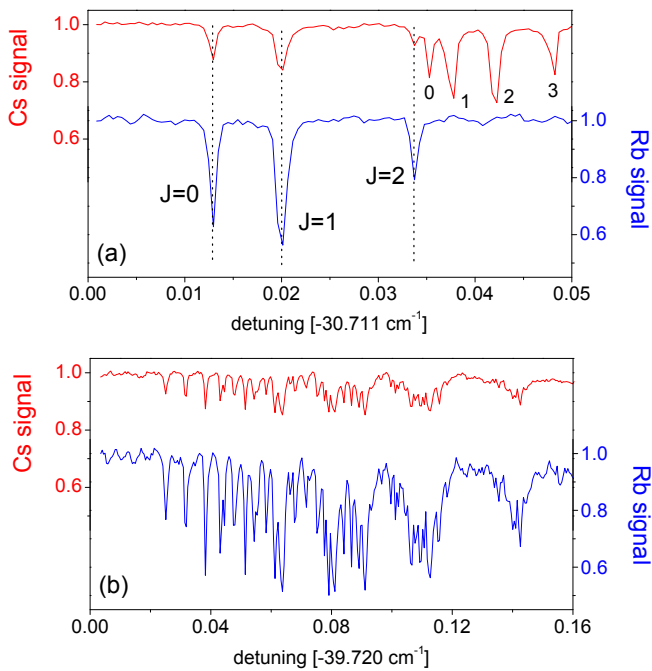


FIG. 2: (Color online) RbCs* PA signals. The PA detuning is specified relative to the $6S_{1/2}$, $F = 3 \rightarrow 6P_{1/2}$, $F' = 3$ transition of Cs at $11178.4172 \text{ cm}^{-1}$. The upper traces (left axes) show the Cs trap population and the lower (right axes) the Rb trap population. (a) The features marked with dashed lines arise from the $J = 0, 1, 2$ rotational components (J is the quantum number associated with the total molecular angular momentum, except nuclear spin) of a RbCs* 0^- vibrational level with an outer turning point at 13.2 \AA . Another rotational series also appears only in the Cs trace, associated with a 0_u^+ level of Cs* having an outer turning point at 24.8 \AA . Of the two, the RbCs* state has a much larger rotational splitting due to its shorter-range character. (b) Resolved hyperfine-rotational substructure of a RbCs* level with $\Omega \neq 0$.

comparison between the observed $\Omega = 0^\pm$ levels, and the best fit from our model. In the 0^- case [Fig. 4(a)], two distinct vibrational series are evident, with spacings on the order of 3 cm^{-1} and 15 cm^{-1} . These are associated with the two different 0^- potentials dissociating to the $6P_{1/2}$ and $6P_{3/2}$ atomic limits [see Fig. 1(b)]. The latter are bound by more than 550 cm^{-1} , and have outer turning points as small as 9 \AA at our detunings; consequently, these features would be difficult to see without our high PA intensity, as their free-bound FCFs are relatively small. Also evident in the figure is a coupling between these two vibrational series, causing a perturbation in the rotational constant when a near-degeneracy occurs. For the 0^+ levels [Fig. 4(b)], the coupling is so much stronger that almost no trace remains of the “unperturbed” vibrational structure, and all levels have a strongly mixed character, as illustrated by the wavefunction in the inset. This type of coupling has been discussed theoretically [24], and was previously observed in 0_u^+ levels of Cs* [12], though it is a much weaker effect in

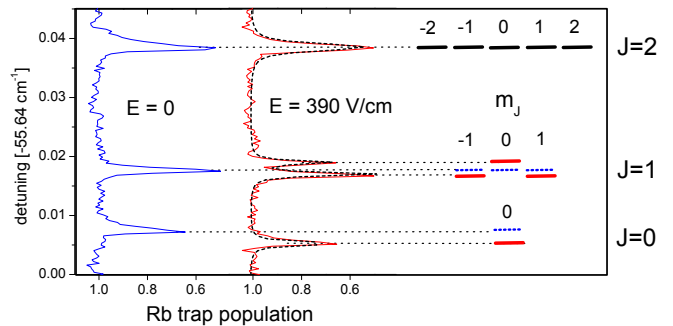


FIG. 3: (Color online) Stark effect in a RbCs* $\Omega = 0^+$ state. The dotted line is a fit of the $E = 390 \text{ V/cm}$ spectrum, based on the expected Stark effect for a diatomic rigid rotor (illustrated schematically on the right) with $\mu_e = 1.3$ Debye.

that system. As a final note, the values we extract from our analysis for the long-range dispersion coefficient C_6 of the RbCs* $A^1\Sigma_0^+$, $b^3\Pi_0$, and $(2)^3\Sigma_0^+$ states [see Fig. 1(a)] all agree with *ab initio* calculations [26] to within a few percent [27, 36].

Using our model of the RbCs* potentials, we can make quantitative estimates of the rate at which ground-state molecules are formed via spontaneous decay in our experiments. For example, taking our observed PA rate of $\sim 1.5 \times 10^8 \text{ s}^{-1}$ on the $\Omega = 0^+$, $J = 1$ resonance at $\Delta = -55.63 \text{ cm}^{-1}$, we predict that $X^1\Sigma^+$ state molecules will be formed in vibrational levels near $v = 62$, bound by almost 1300 cm^{-1} , at a rate of $\sim 5 \times 10^5 \text{ s}^{-1}$ per level [33]. In contrast to the homonuclear case, extremely deeply bound molecules are formed at large rates via decay at a spatially coincident *inner* vibrational turning point of the ground and excited levels [34]. This arises from the shorter-range character of the asymptotic potential as well as the strong 0^+ channel coupling discussed above, which together can produce a large probability density at the inner turning point of the $A^1\Sigma^+$ excited state potential. The resulting deeply bound ground state molecules in $J = 0, 2$ rovibrational levels could be easily transferred with high efficiency to $v = 0, J = 0$ using a single two-photon Raman transition; for example, we calculate that the two FCFs for such a transition, via an intermediate state at $\Delta \sim 3900 \text{ cm}^{-1}$, are both $\geq 10^{-2}$. These transitions could easily be saturated using standard pulsed lasers.

In summary, we have demonstrated photoassociation into polar RbCs* molecular levels in a laser-cooled, dense mixture of ^{85}Rb and ^{133}Cs atoms, at large rates up to $\sim 1.5 \times 10^8 \text{ s}^{-1}$. Analysis of our spectra indicates molecule formation rates via spontaneous decay into deeply bound rovibrational levels of the ground $X^1\Sigma^+$ state as high as $5 \times 10^5 \text{ s}^{-1}$ per level, due to the inherently short-range character of the RbCs* levels we excite. We plan to detect these ground state molecules using resonance-enhanced two-photon ionization [12, 13, 14, 16] and to

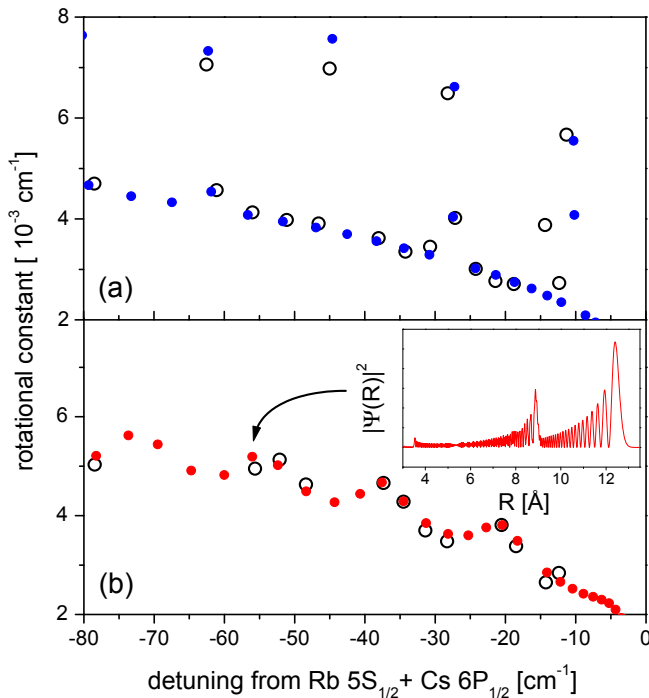


FIG. 4: (Color online) Comparison between observed $\Omega = 0^\pm$ levels (open circles) and those calculated from fitted RbCs* potentials (solid circles). Each point corresponds to a rotational series (e.g. Fig. 2(a)); the horizontal axis gives the energy $E_{v,0}$ of its $J = 0$ component, and the vertical axis its rotational constant B_v , defined by: $E_{v,J} - E_{v,0} = B_v J(J+1)$. (a) 0^- levels; (b) 0^+ levels. Inset: $|\Psi_{b,e}(R)|^2$ for the 0^+ level at $\Delta = -55.63 \text{ cm}^{-1}$, showing its strongly mixed character.

trap them in an optical dipole trap. A two-photon Raman transition from one of the well-populated levels to the rovibrational ground state should allow us to produce a large sample of stable, ultracold polar molecules.

We thank O. Dulieu for information on Cs₂* potentials, and M. Pichler and W. Stwalley for the use of the former's Ph.D. thesis. We acknowledge support from NSF grant EIA-0081332, and the David and Lucile Packard Foundation. T.B. acknowledges funding from the U.S. Office of Naval Research.

[1] D. DeMille, Phys. Rev. Lett. **88**, 067901 (2002).
 [2] M. A. Baranov, *et al.*, Phys. Rev. A **66**, 013606 (2002).
 [3] K. G3ral, L. Santos, and M. Lewenstein, Phys. Rev. Lett. **88**, 170406 (2002).
 [4] S.A. Kivelson, E. Fradkin, and V.J. Emery, Nature **393**, 550 (1998).
 [5] E. Bodo, F. Gianturco, and A. Dalgarno, J. Chem. Phys. **116**, 9222 (2002).
 [6] A.V. Avdeenkov and J. L. Bohn, Phys. Rev. Lett. **90**, 043006 (2003).
 [7] M. Kozlov and L. Labzowsky, J. Phys. B **28**, 1933 (1995).

[8] J.D. Weinstein, *et al.*, Nature **395**, 148 (1998).
 [9] H.L. Bethlem, *et al.*, Nature **406**, 491 (2000).
 [10] J.L. Bohn, A.V. Avdeenkov, and M.P. Deskevich, Phys. Rev. Lett. **89**, 203202 (2002).
 [11] J.L. Bohn, Phys. Rev. A **63**, 052714 (2001).
 [12] C.M. Dion, *et al.*, Phys. Rev. Lett. **86**, 2253 (2001).
 [13] C. Gabbanini *et al.*, Phys. Rev. Lett. **84**, 2814 (2000); D. Heinzen *et al.*, unpublished.
 [14] A. N. Nikolov *et al.*, Phys. Rev. Lett. **84**, 246 (2000).
 [15] R. Wynar, *et al.*, Science **287**, 1016 (2000).
 [16] F.K. Fatemi, *et al.*, Phys. Rev. A **66**, 053401 (2002).
 [17] C. Chin, *et al.*, Phys. Rev. Lett. **90**, 033201 (2003).
 [18] E.A. Donley, *et al.*, Nature **417**, 529 (2002); C.A. Regal, *et al.*, Nature **424**, 47 (2003); J. Herbig, *et al.*, Science **301**, 1510 (2003); S. Jochim, *et al.*, cond-mat/0308095; J. Cubizolles, *et al.*, cond-mat/0308018; S. D3urr, *et al.*, cond-mat/0307440; K.E. Strecker, G.B. Partridge, and R.G. Hulet, Phys. Rev. Lett. **91**, 080406 (2003); K. Xu, *et al.*, cond-mat/0310027.
 [19] S. Kotochigova, P. S. Julienne, and E. Tiesinga, Phys. Rev. A **68**, 022501 (2003).
 [20] H. Wang and W.C. Stwalley, J. Chem. Phys. **108**, 5767 (1998).
 [21] J. P. Shaffer, W. Chalupczak, and N. P. Bigelow, Phys. Rev. Lett. **82**, 1124 (1999); H. Wang, Bull. Am. Phys. Soc. **48**, J1.025 (2003).
 [22] Photoassociation of ⁶Li⁷Li* has been observed in: U. Schl3oder, *et al.*, Phys. Rev. A **66**, 061403(R) (2002). However, due to the identical nuclear charges this molecule has a negligible μ_e , and due to the small isotope shift the PA is essentially homonuclear in character.
 [23] A. Simoni, *et al.*, Phys. Rev. Lett. **90**, 163202 (2003); B. Damski, *et al.*, Phys. Rev. Lett. **90**, 110401 (2003).
 [24] O. Dulieu and F. Masnou-Seeuws, J. Opt. Soc. Am. B **20**, 1083 (2003), and references therein.
 [25] J.L. Bohn and P.S. Julienne, Phys. Rev. A **60**, 414 (1999).
 [26] M. Marinescu and H. R. Sadeghpour, Phys. Rev. A **59**, 390 (1999).
 [27] See EPAPS Document No. [] for more details and a table of observed resonances.
 [28] T. Bergeman, *et al.*, J. Chem. Phys. **117**, 7491 (2002), and references therein.
 [29] W. Ketterle, *et al.*, Phys. Rev. Lett. **70**, 2253 (1993).
 [30] M. H. Anderson, *et al.*, Phys. Rev. A **50**, R3597 (1994).
 [31] A.R. Allouche, *et al.*, J. Phys. B **33**, 2307 (2000).
 [32] T. Bergeman, *et al.*, Phys. Rev. A **67**, 050501 (2003).
 [33] We neglect stimulated processes (such as photodissociation) which may also deplete the excited levels, since we observe no PA-induced broadening at the few MHz level.
 [34] One could also use an $\Omega = 1$ level. These in general contain an admixture of the $(1)^1\Pi$ state, whose inner turning point is predicted to occur at longer range, resulting in decay rates to $X^1\Sigma^+ v \sim 18$ of $3 \times 10^6 \text{ s}^{-1}$ [27].
 [35] The lower atom number and density and higher temperature of the Cs MOT resulted from its higher trapping laser intensity; this was used to keep its intrinsic losses high, to reduce its depletion by the many Cs₂* resonances.
 [36] We are presently unable to assign definitive uncertainties to these values, however, due to the large parameter space and limited experimental data [27].